Cleveland State University
EngagedScholarship@CSU

MSL
ACADEMIC ENDEAVORS

Mechanical Engineering Faculty Publications | Mechanical Engineering Department

11-15-2009

Intermittent Behaviour of a Cracked Rotor in the Resonance Region

Grzegorz Litak
University of Lublin, g.litak@pollub.pl

Jerzy T. Sawicki
Cleveland State University, j.sawicki@csuohio.edu

Follow this and additional works at: https://engagedscholarship.csuohio.edu/enme_facpub


Part of the Mechanical Engineering Commons

How does access to this work benefit you? Let us know!

Publisher's Statement

NOTICE: this is the author's version of a work that was accepted for publication in Chaos, Solitons & Fractals. Changes resulting from the publishing process, such as peer review, editing, corrections, structural formatting, and other quality control mechanisms may not be reflected in this document. Changes may have been made to this work since it was submitted for publication. A definitive version was subsequently published in Chaos, Solitons & Fractals, 42, 3, (11-15-2009); dx.doi.org/10.1016/j.chaos.2009.03.050

Original Citation

Grzegorz Litak, Jerzy T. Sawicki. (2009). Intermittent behaviour of a cracked rotor in the resonance region. Chaos, Solitons & Fractals, 42(3), 1495-1501, doi: dx.doi.org/10.1016/j.chaos.2009.03.050.

This Article is brought to you for free and open access by the Mechanical Engineering Department at EngagedScholarship@CSU. It has been accepted for inclusion in Mechanical Engineering Faculty Publications by an authorized administrator of EngagedScholarship@CSU. For more information, please contact library.es@csuohio.edu.

Intermittent behaviour of a cracked rotor in the resonance region

Grzegorz Litak [a], Jerzy T. Sawicki [b,*]

[a] Department of Applied Mechanics, Technical University of Lublin, Nadbystrzycka 36, PL-20-618 Lublin, Poland
[b] Cleveland State University, Department of Mechanical Engineering, Cleveland, OH 44115, USA

1. Introduction

In many technical devices and machines possessing rotors, i.e. turbines, pumps, compressors, etc., their actual dynamic condition determines their proper and safe operation. Often, these machines have to work over the extended periods of time in various temperature regimes under large variable loading. As a consequence, the components of the machine are exposed to potential damage, such as for example transverse crack [1,2]. For reliable and safe operation of such machines their rotors should be systematically monitored for presence of cracks and tested using non-destructive tests or vibration based techniques [21]. Structural health assessment of the rotating components may be performed by examining the dynamical response of the system subjected to external excitation applied to the rotating shaft. Such a strategy requires solution and study of the dynamical behaviour of the rotor [3,4]. The main difference between the cracked and uncracked rotors can appear in the region of internal or combination resonances [5,6]. One should notice that the dynamics of the rotor is related to the coupling of torsional and lateral vibrations and the whole system is nonlinear. The crucial point is related to the model of the "breathing" crack, indicating that cracks involve additional parametric excitations with the frequency equal to an angular velocity of the rotor rotation [8,7]. The crack introduces extra nonlinearity terms and produces coupling terms of lateral and torsional modes.

Tondl [9], Cohen and Porat [10] and Bernasconi [11] showed that typical lateral excitations, such as unbalance, may result in both lateral and torsional responses of uncracked rotor. Continuing these works Muszynska et al. [12] and Bently et al. [13] discussed rotor coupled lateral and torsional vibrations due to unbalance. Their experimental results exhibited the existence of significant torsional vibrations, due to coupling with the lateral modes. Further reported works have used this coupling under external excitation as a means to identify the presence of cracks [14,15]. It has become clear that the spectral components of the shaft response under radial excitation can be used to identify the presence of transverse shaft cracks. In particular, Iwatsubo et al. [16] considered the vibrations of a slowly rotating shaft subject to either periodic or impulsive excitation. They identified specific harmonics in the response spectrum, which are combinations between the rotation speed

* Corresponding author.
E-mail addresses: g.litak@pollub.pl (G. Litak), j.sawicki@csuohio.edu (J.T. Sawicki).

and excitation frequency and they can be used to detect the presence of the crack. Also, Iwatsubo et al. [16] noted that the sensitivity of the response to the magnitude of the damage depends on the value of the excitation frequency chosen for the detection. Finally, Ishida and Inoue [17] considered the response of a horizontal rotor to harmonic external torques. Furthermore, Sawicki et al. [18,19,7] examined transient response of the cracked rotor, including the stalling effect under the constant driving torque.

In this paper, we continue these investigations. By applying the external harmonic torque excitation we show the characteristic features of internal resonances leading to quasi-periodic and non-periodic types of motion.

2. The model and equations of motion

The model of the Jeffcott rotor, which is by a definition limited to a rotating mass disc and massless rotating elastic shaft, is presented in Fig. 1.

The angular position of the unbalance vector can be written as

$$\theta(t) = \omega t + \psi(t) + \beta, \psi \tag{1}$$

where ω is a constant spin speed of the shaft, $\psi(t)$ is a torsional angle, while β is the fixed angle between the unbalance vector and the centerline of the transverse shaft surface crack. It should be noted that

$$\dot{\theta} = \dot{\Phi} = \omega + \dot{\psi}, \psi \quad \ddot{\theta} = \ddot{\psi}, \psi \tag{2}$$

where Φ is the spin angle of the rotor (Fig. 1).

The kinetic T and potential U energies for the rotor system subjected to lateral and torsional vibrations can be expressed as follows:

$$T = \frac{1}{2} J_p \dot{\theta}^2 + \frac{1}{2} M(\dot{z}^2 + \dot{y}^2) + \frac{1}{2} M\epsilon^2 \dot{\theta}^2 + M\epsilon\dot{\theta}(-\dot{z}\sin\theta + \dot{y}\cos\theta) \tag{3}$$

$$U = \frac{1}{2}\{zy\}\mathbf{K}_l \begin{Bmatrix} z \\ y \end{Bmatrix} + \frac{1}{2} k_t \psi^2, \psi \tag{4}$$

where the stiffness matrix reads

$$\mathbf{K}_l = \begin{bmatrix} k_{zz} & k_{zy} \\ k_{yz} & k_{yy} \end{bmatrix}. \psi \tag{5}$$

The coupled equations for transverse and torsional motion for the rotor system take the following form:

$$M\ddot{z} + C_l\dot{z} + k_{zz}z + k_{zy}y = F_z + M\epsilon\left(\ddot{\psi}\dot{\theta}^2\cos\theta + \ddot{\theta}\sin\theta\right) \tag{6}$$

$$M\ddot{y} + C_t\dot{z} + k_{yz}z + k_{yy}y = F_y + M\epsilon\left(\ddot{\psi}\dot{\theta}^2\sin\theta + \ddot{\theta}\cos\theta\right) \tag{7}$$

$$J_p\ddot{\psi} + C_t\dot{\psi} + \epsilon C_l(\dot{z}\sin\theta - \dot{y}\cos\theta) - \epsilon(F_z\sin\theta - F_y\cos\theta) + \epsilon\left[\ddot{\psi}(k_{zz}z + k_{zy}y)\sin\theta - (k_{yz}z + k_{yy}y)\cos\theta\right] + \frac{\partial U}{\partial\psi} = T_e, \psi \tag{8}$$

where M and J_p is the mass and mass moment of inertia of the disk, while ϵ is eccentricity of the disk. F_z and F_y are the external forces (including gravity) in z and y directions, respectively, C_l and C_t are lateral and torsional damping coefficients, T_e is an external torque. In our case

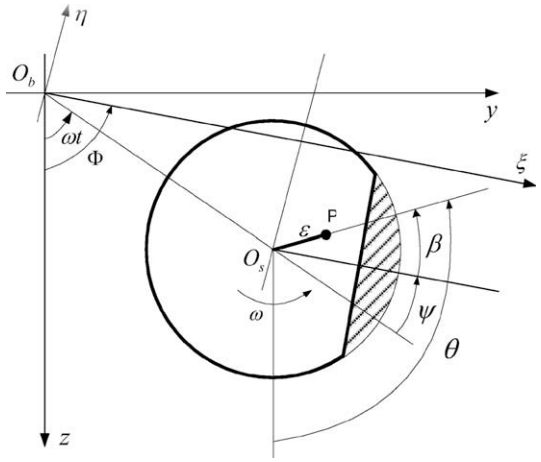

Fig. 1. Schematic plot of the cracked Jeffcott rotor [7].

$$F_z = -Mg, \psi \quad F_y = 0, \psi \quad T_e = T_0 \sin(\omega_e t). \psi \tag{9}$$

where g is the gravitational acceleration, T_0 and ω_e are amplitude and frequency of the external torque, respectively.

The stiffness matrix for a Jeffcott rotor with a cracked shaft in rotating coordinates can be written as:

$$\mathbf{K}_R = \begin{pmatrix} k_\xi & 0 \\ 0 & k_\eta \end{pmatrix} = \begin{pmatrix} k & 0 \\ 0 & k \end{pmatrix} - f(\Phi) \begin{pmatrix} \Delta k_\xi & 0 \\ 0 & \Delta k_\eta \end{pmatrix}, \psi \tag{10}$$

where the first matrix, on the left hand side, refers to the stiffness of the uncracked shaft, and the second defines the variations in shaft stiffness k_ξ and k_η in ξ and η directions, respectively. The function $f(\Phi)$ is a crack steering function which depends on the angular position of the crack Φ. The hinge model of the crack might be an appropriate representation for very small cracks, Mayes and Davies [20] proposed a model with a smooth transition between the opening and closing of the

Table 1
Parameters for a simple-supported Jeffcott rotor with a crack.

Disk mass, M	3 kg
Disk polar moment of inertia, J_p	0.01 kg m^2
Eccentricity of the disk, $\epsilon\psi$	2.2×10^{-5} m
Torsional natural frequency, ω_t	630 rad/s
Lateral natural frequency, ω_t	210 rad/s
Shaft lateral stiffness, k	$k = \omega_l^2 M$
Shaft torsional stiffness, k_t	$k_t = \omega_t^2 J_p$
Damping ratio in lateral direction, ξ_l ($C_l = 2\xi_l M\omega_l$)	0.008
Damping ratio in torsional direction, ξ_t ($C_t = 2\xi_t J_p \omega_t$)	0.0006
External torque amplitude, T_0	800 Nm
External torque amplitude, ω_e	$\in [100, 250]$ rad/s
Relative stiffness change caused by cracks $\frac{\Delta k_\xi}{k}$ ($\Delta k_1 = \frac{7}{6}\Delta k_\xi/k$, $\Delta k_2 = \frac{5}{6}\frac{\Delta k_\xi}{k}$)	0.4

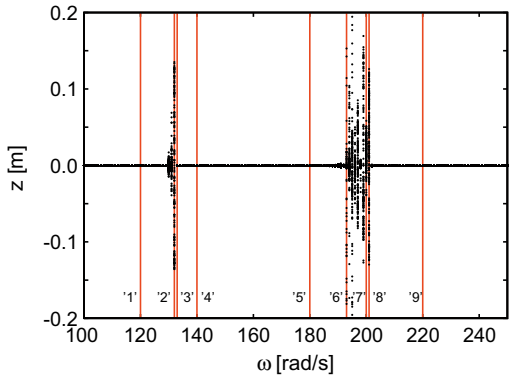

Fig. 2. Bifurcation diagram of the cracked rotor. The numbers '1'–'9' correspond to ω = 120, 132, 133, 140, 180, 193, 200, 201, and 220 rad/s.

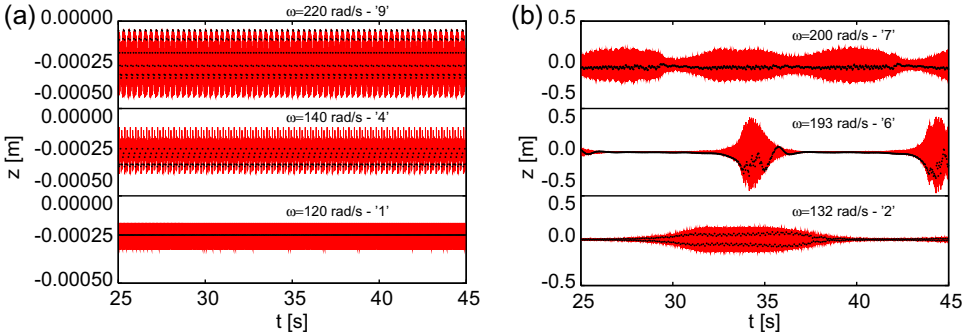

Fig. 3. Time histories of displacement in the vertical direction (a) for ω = 120, 140, 220 rad/s (small amplitude periodic vibrations) and (b) for ω = 132, 193, 200 rad/s (intermittent vibrations). Black points shows stroboscopic points. Numbers '1', '4', '9', '2', '6', and '7' indicate the corresponding values in the bifurcation diagram (Fig. 2).

crack that is more adequate for larger cracks. In this case the crack steering function, or the Mayes function, takes the following form:

$$f(\Phi) = \frac{1+\cos(\Phi)}{2}.\psi \tag{11}$$

The stiffness matrix for a Jeffcott rotor with a cracked shaft in inertial coordinates, $\mathbf{K}_I$ is derived as

$$\mathbf{K}_I = \mathbf{T}\mathbf{K}_R\mathbf{T}^{-1},\psi \quad \mathbf{T} = \begin{pmatrix} \cos\Phi & -\sin\Phi \\ \sin\Phi & \cos\Phi \end{pmatrix},\psi \tag{12}$$

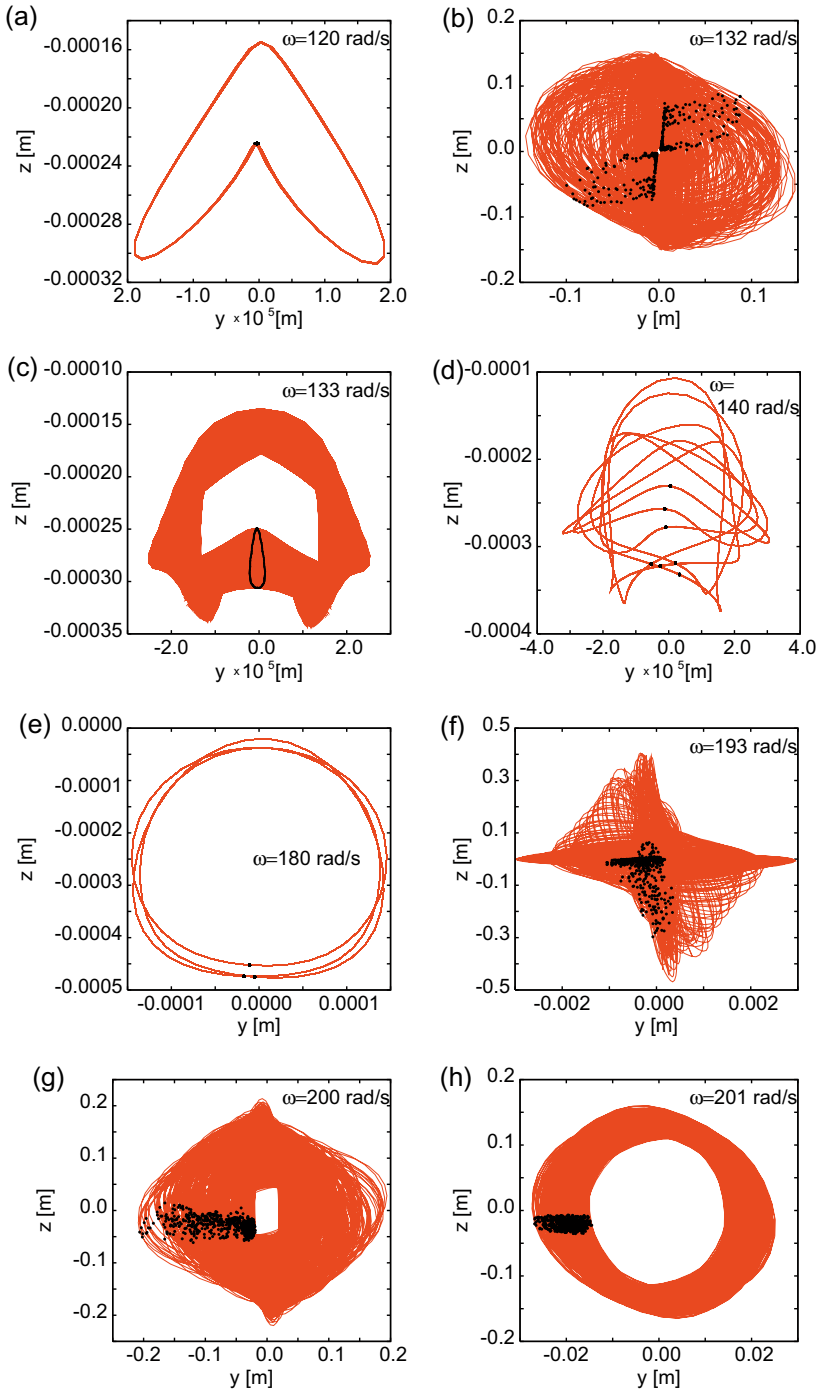

Fig. 4. Phase diagram projections into z–y plane for few values of speed velocities (ω = 120, 132, 133, 140, 180, 193, 200, and 201).

where

$$\Delta k_1 = \overleftarrow{\frac{\Delta k_\xi + \Delta_\eta}{2}}.\psi \;\; \Delta k_1 = \overleftarrow{\frac{\Delta k_\xi - \Delta_\eta}{2}}.\psi \tag{13}$$

Consequently after [7]:

$$\frac{\partial U}{\partial \psi} = -\frac{k}{4}\frac{\partial f(\Phi)}{\partial \psi}\left[(\Delta k_1 + \Delta k_2 \cos 2\Phi)z^2 + 2zy\Delta k_2 \sin 2\Phi + (\Delta k_1 - \Delta k_2 \cos 2\Phi)y^2\right] + \overleftarrow{\frac{f(\Phi)k\Delta k_2}{2}}\left[z^2 \sin 2\Phi - 2zy\cos 2\Phi - y^2 \sin 2\Phi\right] + k_t\psi.\psi \tag{14}$$

3. Results of simulations

Assuming the example of simply supported steel shaft, with a disc at the center and a transverse crack located near the disk, we applied Eqs. (6)–(8) and performed the simulations. The parameters of the examined system are shown in the Table 1. Simulations were done using the Euler integration procedure with a integration step $\delta t = 2\pi/(36000\omega)$ and a sampling time $\Delta t = 1000\delta t$.

The results for the range of rotational velocities $\omega \in [100,250]$ are presented in the bifurcation diagram (Fig. 2). One can see that the resonances appear as they are expected just below the lateral natural frequency and slightly above the half of lateral natural frequency, which one would expect for a non-linear system of this kind. Spanning the rotor spin speed in the range of 145–149 rad/s and 216–234 rad/s, reveals the presence of a wide variety of the excited response characteristics. To explain the nature of vibrations in the regions of resonance we focused on the specific frequencies denoted by '1'–'9' for the corresponding values ω = 120, 132, 133, 140, 180, 193, 200, 201, and 220 rad/s. In Fig. 3a, we show the time histories of displacement in the vertical direction for nonresonat cases ω = 120, 140, 220 rad/s. Black points are stroboscopic points plotted with the rotation frequency ω. Note that all three considered here cases indicate periodic vibrations with a small amplitude. On the other hand in Fig. 3b we show the resonant time series with rotation velocities ω = 132, 200, 201 rad/s. In contrary to the previous cases the displacement z can be large. Interestingly it increases after small laminar behaviour with a relatively small amplitude. Note that in both panels the numbers '1', '4', '9', '2', '6', and '7' indicate the corresponding values ω in the bifurcation diagram (Fig. 2).

To shed some more light into the lateral modes we plotted, in Fig. 4a–h the phase diagram projections into z–y plane are plotted for few values of speed velocities (ω = 120, 132, 133, 140, 180, 193, 200, and 201). Black points indicate the corresponding Poincaré maps. In cases of nonresonant vibrations (Fig. 4a,d,e) of small amplitudes we observe with closed lines and a number of singular black points indicating periodic motion. Interestingly in Fig. 4c the Poincaré map show a line instead of points indicating the quasiperiodic character of motion. The rest of plots (Fig. 4b,f, and g) have non-periodic character. while Fig. 4h has features of moth quasi-periodic and non-periodic. Note that Fig. 4b, f, g, and h look like chaotic attractors, however to tell more about the non-periodic beats nature one should perform standard calculations of Lyapunov exponents or correlation dimension analysis.

Finally in Fig. 5 we plot the time histories of torsional angular displacements (ω = 132, 193, 200, 201). Black points shows stroboscopic points. Numbers '6', '7', '8', '2' indicate the corresponding values in the bifurcation diagram (Fig. 1). These plots shows the relaxation nature of the torsional oscillations. This is consistent with results for intermittent lateral oscillations presented in Fig. 3. Such an intermittent behaviour can be presented by temporal frequency diagram [22,23] which can be given by the wavelet power spectra [24]. In Fig. 6, one clearly see the laminar (periodic) interplay with turbulent (chaotic) regions. Note that for smaller rotation velocities we observe longer laminar intervals.

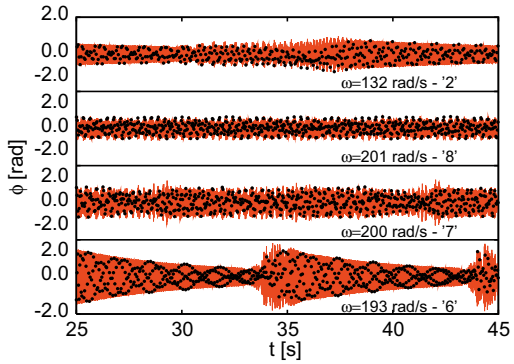

Fig. 5. Time histories of torsional angular displacements ϕ for intermittent oscillations (ω = 132, 193, 200, 201). Black points shows stroboscopic points. Numbers '6', '7', '8', '2' indicate the corresponding values in the bifurcation diagram (Fig. 1).

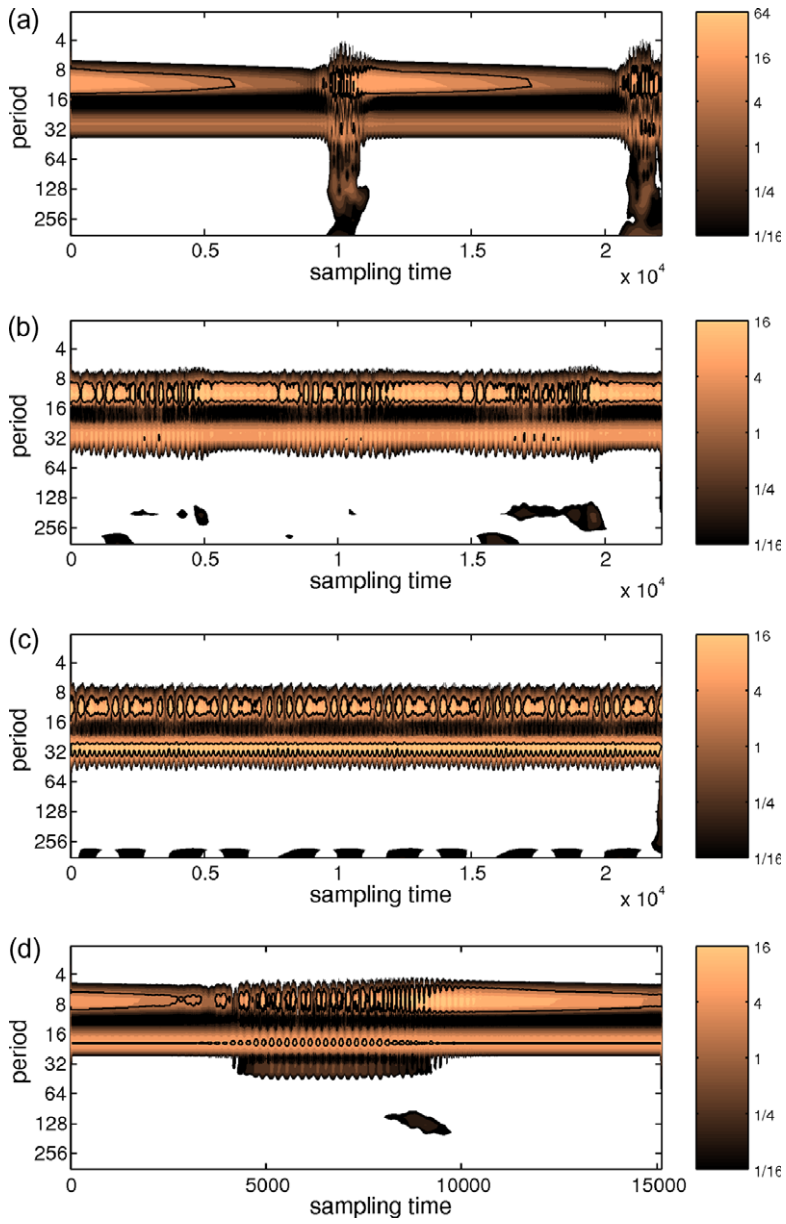

Fig. 6. Wavelet power spectra for torsional angular displacements ϕ; $\omega = 193, 200, 201, 132$ for (a), (b), (c), and (d); respectively. Note, the logarithmic colour scale on the right hand side. White regions in figures (a–d) indicate that power spectrum values exceed the scale.

4. Discussion and conclusions

Using a simple model of the breathing crack we have showed that the response to periodic torque applied at the ends of rotating shaft is complex. In our results, we observe on one hand the multi-frequency synchronization, and on the other hand quasi-periodic motion and nonlinear beats in the regions of resonances. Especially the beats are characteristic as far as the nonlinear coupling of lateral and torsional modes induced by the crack is concerned. The beats are visible in both channels. They are also the signatures of interplay of external and parametric excitations, which arise from the crack existence. Interestingly the beats causing the intermittency of the laminar phases introduce the non-periodic element of vibrations. The chaotic nature of such dynamic response of the rotor system exceeds the present report and will be discussed in detail in a future publication.

Acknowledgments

G.L. thank Dr. Michael Scheffler for helpful discussions. This research has been partially funded by NASA's "Research Opportunities in Aeronautics", grant number NNX08AC31A, and by the Polish Ministry for Science and Higher Education.

References

[1] Gasch R. Dynamic behavior of a simple rotor with a cross-sectional crack. In: Vibrations in rotating machinery. The Institution of Mechanical Engineers; 1976. p. 123–8 [Paper C178/76].
[2] Gasch R. A survey of the dynamic behavior of a simple rotating shaft with a transverse crack. J Sound Vibr 1993;160:313–32.
[3] Dimarogonas AD. Vibration of cracked structures: a state of the art review. Eng Fract Mech 1996;55:831–57.
[4] Wauer J. Dynamics of cracked rotors: a literature review. Appl Mech Rev 1990;43(1):13–8.
[5] Plaut RH, Wauer J. Parametric, external, and combination resonances in coupled flexural and torsional oscillations of an unbalanced rotating shaft. J Sound Vibr 1995;183:889–97.
[6] Chondros TG, Dimarogonas AD. A consistent cracked bar vibration theory. J Sound Vibr 1997;200:303–13.
[7] Sawicki JT, Wu X, Gyekenyesi AL, Baaklini G. Application of nonlinear dynamics tools for diagnosis of cracked rotor vibration signatures. In: Proc of SPIE's int symposium on smart structures and materials. San Diego, California: 2005.
[8] Penny JET, Friswell MI. Simplified modelling of rotor cracks. In: Proc of ISMA 27. Leuven, Belgium: 2002. p. 607–15.
[9] Tondl A. Some problems of rotor dynamics. Prague: Publishing House of Czechoslovakia Academy of Science; 1965.
[10] Cohen R, Porat I. Coupled torsional and transverse vibration of unbalanced rotor. ASME J Appl Mech 1985;52:701–5.
[11] Bernasconi O. Bisynchronous torsional vibrations in rotating shafts. ASME J Appl Mech 1987;54:893–7.
[12] Muszynska A, Goldman P, Bently DE. Torsional/lateral cross-coupled responses due to shafts anisotropy: a new tool in shaft crack detection. In: Proc of IMechE vibrations in rotating machinery. 1992. p. 257–62 [C432–090].
[13] Bently DE, Goldman P, Muszynska A. Snapping torsional response of an anisotropic radially loaded rotor. J Eng Gas Turbines Power 1997;119:397–403.
[14] Collins KR, Plaut RH, Wauer J. Detection of cracks in rotating Timoshenko beams using axial impulses. J Vibr Acoust 1991;113:74–8.
[15] Darpe AK, Gupta K, Chawla A. Coupled bending, longitudinal and torsional vibrations of a cracked rotor. J Sound Vibr 2004;269:33–60.
[16] Iwatsubo T, Arii S, Oks A. Detection of a transverse crack in a rotor shaft by adding external force. Proc IMechE Vibr Rotat Mach 1992;C432/093:275–82.
[17] Ishida Y, Inoue T. Detection of a rotor crack by a periodic excitation. In: Proc of ISCORMA. 2001. p. 1004–11.
[18] Sawicki JT, Wu X, Baaklini G, Gyekenyesi AL. Vibration-based crack diagnosis in rotating shafts during acceleration through resonance. In: Proc of SPIE 10th annual international symposium on smart structures and materials. San Diego, California: 2003.
[19] Sawicki JT, Bently DE, Wu X, Baaklini G, Friswell MI. Dynamic behavior of cracked flexible rotor subjected to constant driving torque. In: Proc of the 2nd international symposium on stability control of rotating machinery. Gdansk, Poland: 2003. p. 231–41.
[20] Mayes IW, Davies WGR. Analysis of the response of a multi-rotor-bearing system containing a transverse crack in a rotor. ASME J Vibr Acoust Stress Reliab Des 1984;106:139–45.
[21] Sawicki JT. Some advances in diagnostics of rotating machinery malfunctions. In: Proc of the int symposium on machine condition monitoring and diagnosis. Tokyo: The University of Tokyo; 2001. p. 138–43.
[22] Sen AK, Litak G, Syta A. Cutting process dynamics by nonlinear time series and wavelet analysis. Chaos 2007;17:023133.
[23] Sen AK, Litak G, Taccani R, Radu R. Wavelet analysis of cycle-to-cycle pressure variations in an internal combustion engine. Chaos, Solitons & Fractals 2008;38:886–93.
[24] Torrence C, Compo GP. A practical guide to wavelet analysis. Bull Am Meteorol Soc 1998;79:6178.

Post-print standardized by MSL Academic Endeavors, the imprint of the Michael Schwartz Library at Cleveland State University, 2014